biomechanics

MDPI

Article

Evaluating the Repeatability of Musculoskeletal Modelling Force Outcomes in Gait among Chronic Stroke Survivors: Implications for Contemporary Clinical Practice

Georgios Giarmatzis [1], Styliani Fotiadou [1,2], Erasmia Giannakou [1], Evangelos Karakasis [1], Konstantinos Vadikolias [2] and Nikolaos Aggelousis [1,*]

[1] Department of Physical Education and Sport Science, Democritus University of Thrace, 69100 Komotini, Greece; ggiarmat@phyed.duth.gr (G.G.); s_fotiadou@yahoo.gr (S.F.); egiannak@phyed.duth.gr (E.G.); ekarakas@pme.duth.gr (E.K.)

[2] Department of Neurology, School of Medicine, University Hospital of Alexandroupolis, Democritus University of Thrace, 68100 Alexandroupolis, Greece; kvadikol@med.duth.gr

* Correspondence: nagelous@phyed.duth.gr

Abstract: This study aims to evaluate the consistency of musculoskeletal modelling outcomes during walking in chronic post-stroke patients, focusing on both affected and unaffected sides. Understanding the specific muscle forces involved is crucial for designing targeted rehabilitation strategies to improve balance and mobility after a stroke. Musculoskeletal modelling provides valuable insights into muscle and joint loading, aiding clinicians in analysing essential biomarkers and enhancing patients' functional outcomes. However, the repeatability of these modelling outcomes in stroke gait has not been thoroughly explored until now. Twelve post-stroke, hemiparetic survivors were included in the study, which consisted of a gait analysis protocol to capture kinematic and kinetic variables. Two generic full body MSK models—Hamner (Ham) and Rajagopal (Raj)—were used to compute joint angles and muscle forces during walking, with combinations of two muscle force estimation algorithms (Static Optimisation (SO) and Computed Muscle Control (CMC)) and different joint degrees-of-freedoms (DOF). The multiple correlation coefficient (MCCoef) was used to compute repeatability for all forces, grouped based on anatomical function. Regardless of models and DOFs, the mean minimum (0.75) and maximum (0.94) MCCoefs denote moderate-to-excellent repeatability for all muscle groups. The combination of the Ham model and SO provided the most repeatable muscle force estimations of all the muscle groups except for the hip flexors, adductors and internal rotators. DOF configuration did not generally affect muscle force repeatability in the Ham–SO case, although the 311 seemed to relate to the highest values. Lastly, the DOF setting had a significant effect on some muscle groups' force output, with the highest magnitudes reported for the 321 and 322 of non-paretic and paretic hip adductors and extensors, knee flexors and ankle dorsiflexors and paretic knee flexors. The primary findings of our study can assist users in selecting the most suitable modelling workflow and encourage the widespread adoption of MSK modelling in clinical practice.

Keywords: stroke; gait; repeatability; musculoskeletal modelling; muscle forces

check for updates

Citation: Giarmatzis, G.; Fotiadou, S.; Giannakou, E.; Karakasis, E.; Vadikolias, K.; Aggelousis, N. Evaluating the Repeatability of Musculoskeletal Modelling Force Outcomes in Gait among Chronic Stroke Survivors: Implications for Contemporary Clinical Practice. *Biomechanics* **2024**, *4*, 333–345. https://doi.org/10.3390/biomechanics4020023

Academic Editors: Pantelis T. Nikolaidis and Enrico Dall'Ara

Received: 13 February 2024
Revised: 19 May 2024
Accepted: 30 May 2024
Published: 1 June 2024

Copyright: © 2024 by the authors. Licensee MDPI, Basel, Switzerland. This article is an open access article distributed under the terms and conditions of the Creative Commons Attribution (CC BY) license (https://creativecommons.org/licenses/by/4.0/).

1. Introduction

Hemiparetic, post-stroke gait research has made a substantial effort to understand neuromuscular deficiencies and enhance post-stroke rehabilitation [1,2]. In particular, rigid-body biomechanics analysis has provided crucial information about how cadence, walking speed, stability and gait symmetry are altered [3–6] in stroke gait, providing an indirect means of assessing individual gait patterns. Moreover, quantitative gait analysis has offered measurable metrics to evaluate hemiplegic gait, such as joint angles and moments [7],

power [8] and work [9–11] to study the effect of orthoses [3] or underlying muscle function. Comprehending the specific forces generated by individual muscles plays a crucial role in designing optimal rehabilitation plans aimed at improving balance and mobility post-stroke. Given the absence of a direct method for measuring muscle forces during movement, employing musculoskeletal modelling is imperative. Musculoskeletal (MSK) modelling addresses the limitations of conventional biomechanical analysis by integrating mathematical approaches to resolve the inherent challenge of distributing external loads among a joint's muscle groups, commonly known as the muscle redundancy problem [12].

MSK modelling techniques have facilitated biomechanics research on deciphering human gait, whether it be healthy or pathological, as a means of improving clinical reasoning and treatment [13]. These usually involve the recruitment of detailed MSK models and rigorous computational simulations of recorded motion, based on rigid-body inverse kinematics and dynamics methods. Their utmost value lies in the wealth of information on muscle and joint function, which can make estimates based on musculotendon length/moment arm [14] and individual muscle forces [15,16] to joint forces [12,17] and cartilage pressure distributions [18]. According to our recent review [19], a variety of MSK modelling methods were used to assess muscle function, optimise ankle–foot orthoses prescription or predict the effect of treatment, demonstrating the power of such analyses to study individual post-stroke gait [20].

The two most common methods include Static Optimisation (SO) and Computed Muscle Control (CMC) [21]. SO calculates muscle forces based on an inverse dynamics approach at each time frame, minimising muscle effort as the sum of squared muscle activations [22]; CMC also utilises SO, however in a recursive step-wise way while trying to find the set of muscle forces that allow the MSK model to follow calculated and dynamically consistent kinematics, which can differ slightly from the original. SO has not been validated in stroke patients, whereas CMC showed varying levels of correlations between simulated and experimental muscle activation profiles during post-stroke late-swing and pre-swing phases [23], while similar results were found by Jansen et al. [24] during the whole gait cycle. Comparisons between muscle force estimations show that CMC generally produces higher values, possibly due to the inclusion of muscle contraction dynamics and passive elements [25]. Nevertheless, SO remains the most preferable muscle-force estimation method [21], being the most efficient and producing similar results to CMC during healthy walking.

There has been no prior assessment of the repeatability of MSK outcomes in the context of stroke-related gait, which builds on the restricted integration of such methods into clinical practice, with the latter attributed to their complexity and skill-demanding characteristics [26]. Consistency in the methods used to calculate muscle forces is crucial for the stroke population exhibiting larger variability on key biomechanical parameters [27]; thus, a proper estimation may represent a stronger validation of the methods. Previous research has shown excellent repeatability for almost all joint angles, moments and powers in the gait of cerebral-palsy [28] and post-stroke patients [29] (the same group used in this study) using open-source software Opensim v. 4.3 [30] and commercial software (Vicon Nexus®) respectively. However, small changes in joint angles or moments can highly impact calculated muscle forces [31–33], but its effect on their repeatability is not yet known, limiting scientific reasoning on the potential smallest treatment effect. Previous work of our group has used Opensim and SO to identify how a training program has impacted lower limb force generation in one patient of the same group of stroke patients used in this study, although our conclusions could have been confounded by the unknown variability/repeatability in muscle force estimations. Also, different MSK models may impose extra variability in estimated parameters, due to discrepancies in defined coordinate systems, number of segments and muscle properties [34,35]. Selection of muscle force estimation algorithms could be another source of variability. To date, only one study researched on reproducibility of muscle forces based on a single model and muscle force estimation algorithm, however only on pedalling exercise on healthy individuals [36].

To address this literature gap, this study builds upon our findings on repeatability of joint angles/moments/powers during post-stroke walking of the same group. It also aims to assess the repeatability of muscle force calculations as derived from two popular full body MSK models with different sets of unlocked knee/ankle DOFs, and the two mostly used and computationally efficient muscle force estimation algorithms, SO and CMC. The main goal is to identify the best possible combination with the highest repeatability among the possible choices to model stroke gait with different research goals.

2. Materials and Methods

2.1. Participants

Twelve post-stroke, hemiparetic survivors were included as part of our previous study [29] (Table 1), consisting of a gait analysis protocol to capture kinematic and kinetic variables. The study was approved by the Institutional Research Ethics Committee of the Democritus University of Thrace and informed consent was obtained from all subjects involved in the study. The criteria for inclusion comprised individuals who had experienced a stroke in the prior 12–18 months; exhibited mild motor impairment without ataxia or sensory deficits; could walk continuously for at least 20 m unaided or without orthoses; demonstrated the capacity to comprehend and adhere to straightforward verbal instructions; lacked any prior history of neuromuscular, musculoskeletal or severe cardiovascular disorders; possessed adequate vision.

Table 1. Patient characteristics.

	Number	**Age**	**Body Mass Index**
male	6	68.2 (5.7)	28.2 (2.7)
female	6	60.8 (10)	31.5 (3.7)

2.2. Motion Capture

Prior to recording, retro-reflective markers were placed on anatomical positions according to the Vicon Plug-in-Gait lower-body protocol [37]. The motion analysis system comprised six infrared cameras (Vicon MX 0306012, Oxford, UK) and two ground embedded force plates (type 9281B11 and 9281CA, Kistler Instruments AG, Winterthur, Switzerland) along a 10 m straight walkway, synchronously recording marker trajectories and ground reaction forces at 100 and 1000 Hz, respectively (Figure 1). The participants attended one session, where they were instructed to walk barefoot along the walkway in their self-selected (natural) speed, alternating directions. To measure their natural walking speed, an electronic timer was employed, and was connected to two photocells positioned 3 m apart at the midpoint of the walkway. A trial was deemed successful if either foot hit one force plate during a full gait cycle (heel strike to ipsilateral heel strike). Finally, five trials for each lower limb were used for further analysis.

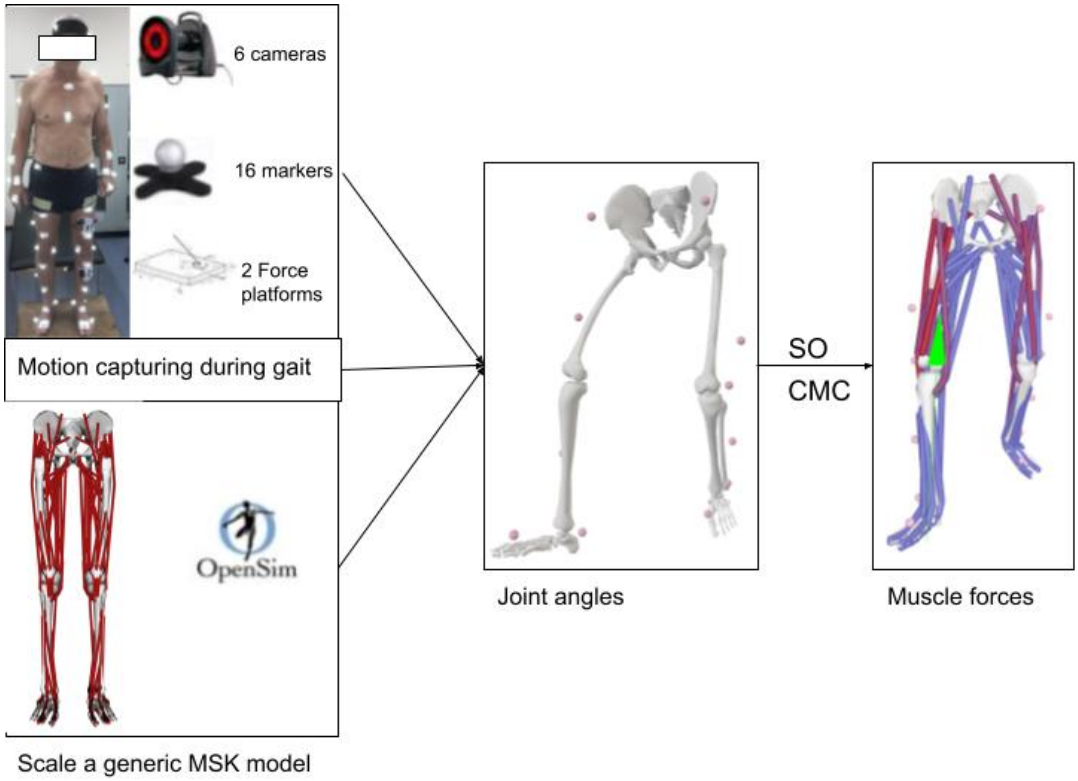


Figure 1. A six-camera Vicon system, sixteen retro-reflective markers and two ground embedded force plates were used for motion capture. For the Opensim analysis, a static trial was recorded to scale the generic lower limb models. Then, recorded marker trajectories (pink spheres) and GRFs (green arrows) were used to calculate joint angles and muscle forces during gait using SO and CMC.

2.3. Musculoskeletal Modelling

2.3.1. Muscle Skeleton Models

Free open-source software Opensim 4.3 [38] was used for all MSK modelling routines. Two generic full body MSK models were employed—Hamner (Ham) [39] and Rajagopal (Raj) [40]—and were linearly scaled to each participant's anthropometry based on a static trial after their torso and hands were condensed to the pelvis (Figure 1). The Ham model incorporates torso and arm segments in the novel model of Delp et al. [41] who developed a lower limb model utilising parameter values for muscle–tendon units primarily acquired from five cadavers. The Raj model builds upon the foundation laid by Arnold et al. [42], who expanded the Delp model by enhancing bone geometry and incorporating muscle architecture based on a broader dataset derived from 21 cadavers. The standard Hill-type model is implemented in both models. Both MSK models have almost similar muscles assigned to the same muscle groups, defined by their anatomical function. The main difference is the definition of the adductor magnus muscle; that is, the Raj model has four instead of three parts as in the Ham model, with the latter including the pectineus muscle, which has a similar function to the magnus proximal of the former. For further information, see Supplementary Material Table S1. Different configurations of unlocked degrees-of-freedom (DOF) were allowed in both models, mainly by keeping all three DOFs at the hip joint and sagittal DOF at the knee and ankle joint, allowing the knee abduction/adduction, rotation and ankle eversion/inversion to vary. Hence, each configuration was named 3-k-l, where k and l are the numbers of knee and ankle DOFs, respectively.

2.3.2. Musculoskeletal Modelling

Joint kinematics were calculated with the Inverse Kinematics Tool by solving a weighted least squares optimisation problem with the goal of minimising marker errors.

The calculated joint angles were used along with ground reaction forces as inputs to compute muscle activations with Static Optimisation (SO) and Computed Muscle Control (CMC) tools in Opensim. In SO, muscle forces are computed at every moment of the movement as a function of the activation, maximal isometric force and moment arm, aiming to instantaneously minimise the total squared muscle activation. A quadratic optimisation criterion was employed, as it has demonstrated the highest concordance between electromyography (EMG) and muscle activations. CMC integrates SO with feedforward and feedback controls to determine muscle activations and, consequently, muscle forces, taking into consideration muscle activation and contraction dynamics [43].

2.4. Data Processing and Statistics

Muscle forces were calculated during each gait cycle, which was defined as the time window between two consecutive ipsilateral heel strikes. Then, all muscle force outcomes were normalised to 101 points using quadratic interpolation with the python package, scipy [44].

Multiple correlation coefficient [45] (MCCoef) was used as a repeatability measure of muscle forces computed among all five gait cycles for each leg (paretic and non-paretic), which were then averaged between all cycles and subjects. MCCoef is a waveform similarity statistical approach typically used to assess repeatability, taking into account the whole curve of a biomechanical outcome. MCCoef values above 0.90 are excellent, values of 0.8–0.9 are good, values of 0.65–0.8 are moderate and values of <0.65 are poor. To avoid the excessive output of results based on a single muscle output, which can be confusing to the average reader, MCCoef was applied after the summation of muscle forces based on their anatomical function and plane of movement. Such categorisation can be crucial to rehabilitation experts who design training programs that, by definition, require muscles to work synergistically.

3. Results

The distribution of the MCCoef values for all muscle groups and sides were not normal, thus the effect of the combination model–DOF–optimisation algorithm was not tested and the discussion about the results will be qualitative only. Maximum (minimum) repeatability measures for each muscle group and side (paretic and non-paretic) are shown in Table 2; they all show excellent repeatability of muscle force calculations, except for the ankle dorsiflexors of the non-paretic side, which showed good repeatability (mean MCCoef = 0.85). Minimum repeatability measures for both sides show generally good-to-moderate repeatability (range: 0.67–0.87) and poor repeatability for the ankle dorsiflexors group (0.64). No meaningful differences between the paretic and non-paretic side have been found. Next, the Hamner model evidently produced the most repeatable results for most muscle groups, except for the hip flexors, adductors and internal rotators. No conclusion can be drawn as to the worst performing model, since both models are almost equally related to minimum repeatability. The most frequent DOF configuration related to higher MCCoef was the simplest 311 (11 out of 20); that is, with only knee flexion/extension and ankle plantarflexion/dorsiflexion. However, other configurations with a focus on knee DOF variations relate to high MCCoef. On the contrary, minimum repeatability is related to the most complex configuration, in which all three knee and two ankle DOFs are free. Moreover, the dominant optimisation routine with the highest repeatability was found to be SO, except for CMC combined with the Raj model in the case of hip adductors. Instead, CMC was found to provide the lowest repeatability for all muscle groups, except the hip flexors. Lastly, the optimal combination of model–DOF–optimisation appears to be Ham–311–SO, providing highly reproducible muscle forces in four cases, being the hip abductors, hip external rotators and ankle dorsiflexors/plantarflexors. The same DOF–SO configuration had excellent reliability with the Raj model in the case of hip flexors.

Table 2. Maximum (minimum) repeatability values and their corresponding model, DOF and optimisation routine for each muscle group and side.

Muscle Group	MCCoef		Model		DOF		Optimisation	
	P	NP	P	NP	P	NP	P	NP
Hip flexors	0.95 (0.80)	0.95 (0.80)	Raj (Ham)	Raj (Ham)	311 (322)	311 (322)	SO (SO)	SO (SO)
Hip extensors	0.96 (0.80)	0.96 (0.75)	Ham (Raj)	Ham (Raj)	331 (332)	331 (332)	SO (CMC)	SO (CMC)
Hip abductors	0.97 (0.87)	0.97 (0.81)	Ham (Raj)	Ham (Raj)	311 (332)	311 (332)	SO (CMC)	SO (CMC)
Hip adductors	0.93 (0.72)	0.91 (0.71)	Raj (Ham)	Raj (Raj)	311 (332)	312 (331)	CMC (CMC)	CMC (SO)
Hip internal rotators	0.94 (0.79)	0.95 (0.80)	Raj (Ham)	Raj (Ham)	321 (332)	321 (332)	SO (CMC)	SO (CMC)
Hip external rotators	0.94 (0.67)	0.93 (0.68)	Ham (Raj)	Ham (Raj)	311 (331)	311 (331)	SO (SO)	SO (SO)
Knee flexors	0.95 (0.77)	0.95 (0.74)	Ham (Raj)	Ham (Ham)	332 (332)	331 (321)	SO (CMC)	SO (CMC)
Knee extensors	0.96 (0.70)	0.95 (0.78)	Ham (Ham)	Ham (Ham)	322 (332)	321 (332)	SO (CMC)	SO (CMC)
Ankle dorsiflexors	0.90 (0.64)	0.85 (0.63)	Ham (Ham)	Ham (Ham)	311 (332)	311 (322)	SO (CMC)	SO (CMC)
Ankle plantarflexors	0.95 (0.77)	0.95 (0.80)	Ham (Raj)	Ham (Raj)	311 (332)	311 (332)	SO (CMC)	SO (CMC)

The combination of Ham–SO also produced excellent repeatability results with more complex DOF configurations in the case of knee flexors/extensors and hip extensors (CMC: 0.95–0.96). Thus, we further explored the effect of the DOF variation on repeatability using the Hamner model and SO optimisation method (Table 3). Changes in peak muscle force output are also reported to offer a broader view as to how DOF variation alters muscle force production per muscle group. Muscle forces are normalised to body weight. The Friedman chi-square test was used to study the effect of DOF on MCCoefs and peak muscle forces after identifying abnormal distributions for almost all variables with the Shapiro–Wilk test. The DOF effect on CMC values was found to be significant ($p < 0.05$) only for the case of knee extensors and ankle dorsiflexors for both sides, whereas the effect on peak muscle forces was found to be significant in the case of non-paretic and paretic hip adductors and extensors, knee flexors and ankle dorsiflexors and paretic knee flexors. Post hoc comparisons were performed (a = 0.05) using a pairwise Mann–Whitney U-test when significant interactions were found. Statistically significant differences of CMC values are reported only for the DOF setting with the highest MCCoef (Table 2). Moreover, statistically significant differences between different DOFs for each muscle group are depicted as letters in the respective figure (Figure 2). The data supporting Figure 2 are included as Supplementary Material (Supplementary Table S2).

Table 3. Maximum (minimum) repeatability values for the Hamner model with SO with the corresponding DOF configurations for each muscle group and side. Symbols denote statistical significance. *: Significant DOF effect, [c] significantly different than 321, [d] significantly different than 322, [e] significantly different than 331, [f] significantly different than 332.

Muscle Group	MCCoef		DOF	
	P	NP	P	NP
Hip flexors	0.94 (0.91)	0.95 (0.89)	311 (331)	311 (332)
Hip extensors	0.96 (0.96)	0.97 (0.94)	331 (321)	331 (332)
Hip abductors	0.92 (0.90)	0.97 (0.95)	311 (332)	311 (332)

Table 3. *Cont.*

Muscle Group	MCCoef		DOF	
	P	NP	P	NP
Hip adductors	0.97 (0.96)	0.91 (0.85)	322 (321)	321 (332)
Hip internal rotators	0.94 (0.91)	0.95 (0.91)	311 (331)	311 (332)
Hip external rotators	0.95 (0.91)	0.93 (0.88)	331 (321)	311 (332)
Knee flexors	0.95 (0.91)	0.96 (0.93)	332 (321)	331 (321)
Knee extensors	0.96 * (0.90)	0.96 * (0.91)	322 [c,e] (332)	321 [f] (332)
Ankle dorsiflexors	0.90 * (0.75)	0.85 * (0.76)	311 [f] (312)	311 [d] (322)
Ankle plantarflexors	0.95 (0.94)	0.96 (0.95)	311 (331)	312 (331)

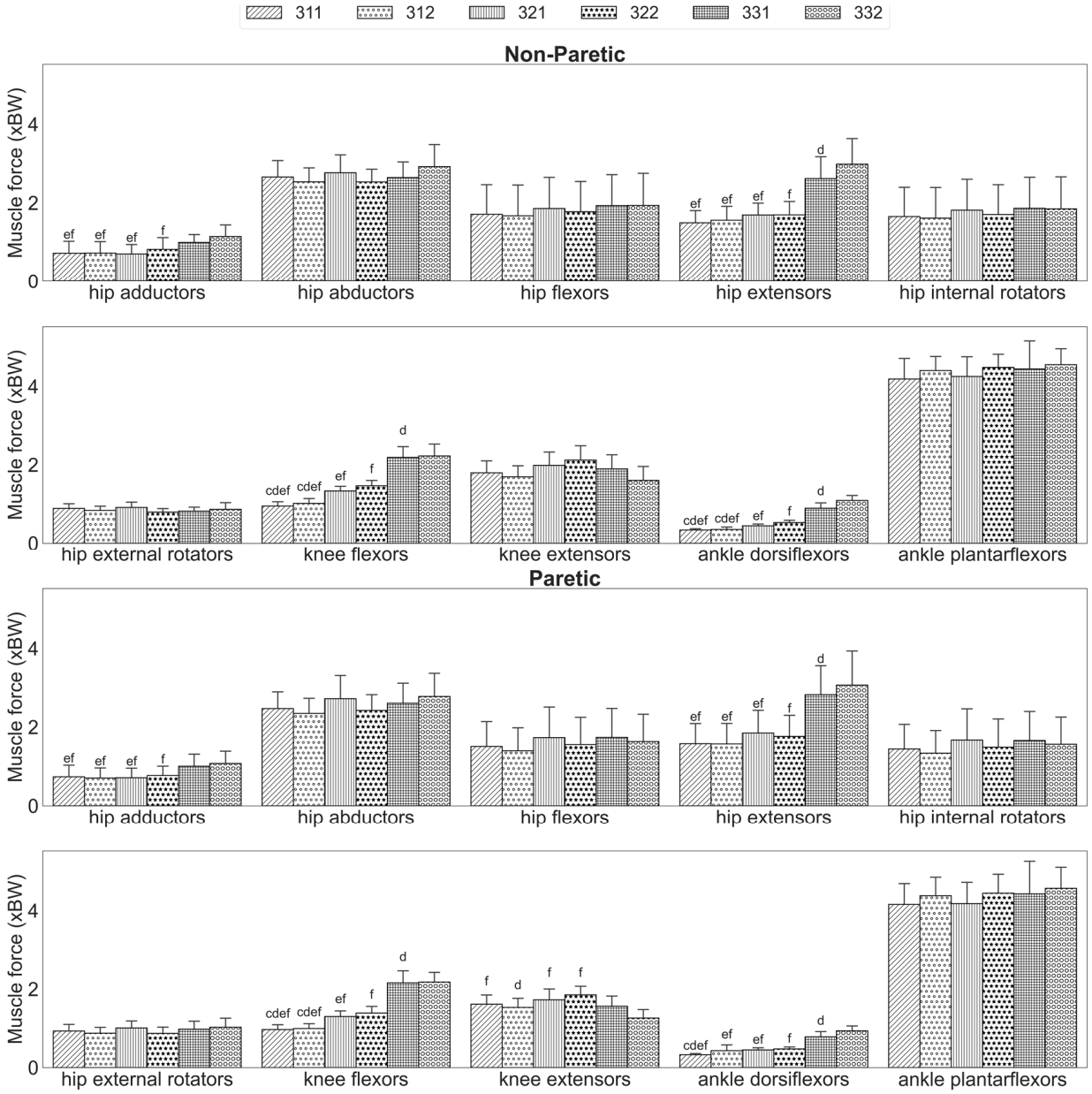


Figure 2. Boxplots showing how mean peak muscle forces per group, when calculated using the Hamner model and SO, are affected by DOF configuration, for the paretic (**above**) and non-paretic side (**below**). Letters denote statistical significance accordingly: c: significantly different than 321, d: significantly different than 322, e: significantly different than 331, f: significantly different than 332.

Lastly, it needs to be reported that the Ham model was more suitable for CMC than SO, with an average of 2 failed (not finished) simulations for the former and 21 failed simulations for the latter, among the different DOF settings. On the contrary, the Raj model produced 0 failed simulations with SO and, on average, 11 failed simulations with CMC.

4. Discussion

MSK modelling has proven to be valuable in addressing functional impairments by estimating parameters that are challenging to measure directly in vivo. It enables the analysis of crucial MSK biomarkers, aiding in optimising rehabilitation, categorising patients, characterising diseases, pre-planning surgeries and designing assistive devices [13]. The current study on post-stroke gait slightly favours the selection of the Hamner over the Rajagopal model as more suitable; however, Static Optimisation yields more repeatable results than Computed Muscle Control. Moreover, different DOF variations can impact repeatability and peak values of muscle force outcomes. These findings could enhance the clinical use of MSK modelling and guide optimal workflow selection.

Low repeatability values (ranging from 0.63 to 0.87) for the two MSK models can be attributed mainly to the number of DOF at the knee and ankle joints and to the optimisation technique. For both models, worst outcomes were reported in the case of complex knee DOF configurations for the majority of muscle groups, where unlocked motion in the transverse and frontal plane is prescribed. The calculation of spatial segmental trajectories at these two planes has been characterised as problematic owing to soft tissue artifacts and crosstalk between the sagittal and frontal planes, thus limiting the calculation of accurate and repeatable knee joint angles. Furthermore, the slightly less repeatable hip transverse angles (around 0.9) reported in our group's previous work may also affect same-plane calculations in the other two joints. Such errors directly influence muscle moment arm [46] and fibre length [47] estimations; hence, the muscle force results. However, the highest repeatability values for more complex DOF configurations are reported in the cases of hip extensors (0.96) and internal rotators (0.95), knee flexors (0.95) and extensors (0.96) (331, 321, 332 and 322, respectively), yet the range between the highest and lowest value denotes good to excellent agreement. Hence, differentiation between DOF configurations for these muscle groups is not possible and it is safe to conclude that the 311 setting could be a valid alternative. When the combination of the Hamner model and Static Optimisation (SO) algorithm was investigated with different DOF settings, the same conclusions were derived from the analysis as above. Lastly, CMC was the optimisation technique with the least repeatable force outcomes, possibly due to the induced changes in prescribed kinematics among intra-subject gait trials as part of the objective function to be minimised [25], which further increased the variability between trials in joint angles already reported by Fotiadou et al. using the same dataset [29].

The muscle group with the minimum highest and lowest (0.85 and 0.63, respectively, for the non-paretic side) repeatability was the ankle dorsiflexors. This finding could be explained by the problematic function of the particular muscle group during the swing phase reported in stroke patients due to a combination of increased plantarflexor passive resistance and/or enhanced activation of the tibialis anterior [48]. Such malfunction seems to be related to high variability in peak ankle dorsiflexion during the stance phase as reported by Yavuzer et al. [49] and higher variability in ankle dorsiflexion during the early swing phase, as reported by Fotiadou et al. [29] in the case of chronic stroke gait. This induces small changes in muscle moment arms between gait cycles and possibly explains the low repeatability of the ankle dorsiflexors' force found in our study.

Our results suggest that peak muscle force estimations using the combination of the Hamner model with SO are generally affected by the DOF configuration being higher when the knee and ankle joint are allowed to move in a frontal and/or transverse plane (see Figure 2 and Supplementary Table S2). In particular, when motion along the knee rotation with adduction/abduction is prescribed (DOF settings: 331 and 332), the muscle forces of the hip extensors, knee flexors and ankle dorsiflexors are the highest for both sides, whereas the lowest occurs in the case of knee extensors. This result is possibly related to the presence of the knee rotation moment and how optimisation chooses to activate certain common knee flexor/hip extensor (see Supplementary Materials Table S1) muscles, such as the biceps femoris long head, semitendinosus and semimembranosus, to counteract this torque, which are highly activated during the early stance phase. Those high activations seem to result in synchronous excessive force estimated in the ankle dorsiflexors, possibly as an effort to counteract the further stabilisation of the tibia in relation to the foot as it externally rotates during the early stance. Future work should research the effect of different knee DOFs on individual muscle force profiles and elucidate this finding.

The estimation of peak muscle forces is significantly dependent on the selected methodology for modelling muscle activation and force generation. In the present study, we employed a Hill-type muscle model, given its established capability to strike an optimal balance between physiological fidelity and computational tractability [50]. The customisation of muscle model parameters was hindered by the absence of specific muscle activation data, consequently constraining our capacity to better simulate stroke patients' movements. The literature indicates that modified Hill models have been leveraged to elucidate upper limb kinematics [51,52], and electromyography data have been utilised to fine-tune Hill-type models for the simulation of both unimpaired [53] and post-stroke ambulation [19]. Additionally, the correlation between EMG signals and muscle forces has been explored through the application of machine learning-based regression analyses [54,55]. Nevertheless, a common limitation across these methodologies is their reliance on hypothetical muscle forces due to the unavailability of direct experimental measurements for validation purposes. Consequently, it becomes apparent that further investigative efforts are imperative to improve the modelling of locomotion post-stroke and to enhance the prediction of related biomechanical outcomes, as well as their reproducibility.

Certain limitations exist in the current study. The limited number of gait cycles and the sample size, non-varying walking paths and the absence of between-session variability calculations are some methodological concerns that may limit the generalisation of the results and conclusions in our study. One of the main shortcomings is the lack of validation of muscle force estimations against experimental data. Direct validation is not possible, as there are no in vivo data available regarding muscle forces during human gait. Alternatively, it is common to compare muscle activations with electromyography (EMG) data [56,57], but there were no available data for the specific patient group. Recent work from our group [58] in another stroke population has shown that SO muscle force activation levels during stroke gait compare well with the synchronous bilateral EMG of eight lower limb muscles, while no particular method of personalisation of the MSK models was followed except the usual linear scaling of segments based on marker placement. Also, consistency in simulation results has given credence to the utilisation of the SO and CMC approach as an investigative tool. Although it may not perfectly capture the muscle coordination observed in stroke patients, when supplemented with subject-specific data and comparative validation against experimental observations, it holds value. Furthermore, no extra level of personalisation, such as EMG-informed modelling or patient-specific geometry, was employed which has been shown to have a huge impact on muscle and joint contact forces, either by changed motor control or muscle properties. Lastly, the low sample size may limit the generalisation of our results and conclusions.

5. Conclusions

To conclude, amongst the combinations, the current work has identified two MSK models with the two most used optimisation methods and six possible DOF configurations with the most repeatable muscle force estimations. Although the Hamner model combined with SO and 311 DOF choice has been shown to provide excellent results (mean highest CMC: 0.93) in most muscle groups compared to other DOFs, readers are encouraged to try other DOF settings as well. However, they should bear in mind that this model was not as repeatable in terms of successful SO in many trials as the Rajagopal model, which is crucial information if population modelling is part of the research. Altogether, MSK modelling can provide highly repeatable results in terms of muscle force estimations and can be advocated for extended usage in clinical research.

Supplementary Materials: The following supporting information can be downloaded at: https://www.mdpi.com/article/10.3390/biomechanics4020023/s1, Table S1: Muscles included in the respective muscle groups for both MSK models; Table S2: Mean and standard deviation values of peak muscle forces, calculated using the Ham model with SO with different DOF settings. Muscle groups with a significant DOF effect setting are in bold.

Author Contributions: Conceptualisation, N.A., G.G. and K.V.; methodology, E.G., S.F., E.K. and G.G.; formal analysis, E.G., S.F., E.K. and G.G.; resources, N.A.; data curation, G.G. and E.K.; writing—original draft preparation, G.G.; writing—review and editing, E.G. and S.F.; visualisation, G.G.; supervision, N.A.; project administration, K.V.; funding acquisition K.V. and N.A. All authors have read and agreed to the published version of the manuscript.

Funding: We acknowledge the support of the work at hand by the project "Study of the interrelationships between neuroimaging, neurophysiological and biomechanical biomarkers in stroke rehabilitation (NEURO-BIO-MECH in stroke rehab)" (MIS 5047286), which is implemented under the Action "Support for Regional Excellence"—Operational Program "Competitiveness, Entrepreneurship and Innovation" (NSRFm2014-2020), under the auspices of Greece and the European Union (European Regional Development Fund).

Institutional Review Board Statement: The study was conducted in accordance with the Declaration of Helsinki and approved by the Institutional Ethics Committee of the Democritus University of Thrace.

Informed Consent Statement: Informed consent was obtained from all subjects involved in the study.

Data Availability Statement: The data and results are available upon request to interested researchers.

Conflicts of Interest: The authors declare no conflicts of interest. The funders had no role in the design of the study; in the collection, analyses or interpretation of data; in the writing of the manuscript; or in the decision to publish the results.

References

1. Belda-Lois, J.-M.; Horno, S.M.; Bermejo-bosch, I.; Moreno, J.C.; Pons, J.L.; Farina, D.; Iosa, M.; Molinari, M.; Tamburella, F.; Ramos, A.; et al. Rehabilitation of gait after stroke:a top down approach. *J. Neuroeng. Rehabil.* **2011**, *8*, 66. [CrossRef] [PubMed]
2. Balaban, B.; Tok, F. Gait Disturbances in Patients with Stroke. *PM R J. Inj. Funct. Rehabil.* **2014**, *6*, 635–642. [CrossRef] [PubMed]
3. Ferreira, L.A.B.; Neto, H.P.; Grecco, L.A.C.; Christovão, T.C.L.; Duarte, N.A.C.; Lazzari, R.D.; Galli, M.; Oliveira, C.S. Effect of ankle-foot orthosis on gait velocity and cadence of stroke patients: A systematic review. *J. Phys. Ther. Sci.* **2013**, *25*, 1503–1508. [CrossRef] [PubMed]
4. Von Schroeder, H.P.; Coutts, R.D.; Lyden, P.D.; Billings, E.; Nickel, V.L. Gait parameters following stroke: A practical assessment. *J. Rehabil. Res. Dev.* **1995**, *32*, 25. Available online: https://pubmed.ncbi.nlm.nih.gov/7760264/ (accessed on 25 April 2024). [PubMed]
5. Nardone, A.; Godi, M.; Grasso, M.; Guglielmetti, S.; Schieppati, M. Stabilometry is a predictor of gait performance in chronic hemiparetic stroke patients. *Gait Posture* **2009**, *30*, 5–10. [CrossRef] [PubMed]
6. Lauziere, S.; Betschart, M.; Aissaoui, R.; Nadeau, S. Understanding spatial and temporal gait asymmetries in individuals post stroke. *Int. J. Phys. Med. Rehabil.* **2014**, *2*, 201. Available online: https://www.longdom.org/abstract/understanding-spatial-and-temporal-gait-asymmetries-in-individuals-post-stroke-45980.html (accessed on 9 June 2022).

7. Boudarham, J.; Roche, N.; Pradon, D.; Bonnyaud, C.; Bensmail, D.; Zory, R. Variations in Kinematics during Clinical Gait Analysis in Stroke Patients. *PLoS ONE* **2013**, *8*, e66421. [CrossRef] [PubMed]
8. Peterson, C.L.; Hall, A.L.; Kautz, S.A.; Neptune, R.R. Pre-swing deficits in forward propulsion, swing initiation and power generation by individual muscles during hemiparetic walking. *J. Biomech.* **2010**, *43*, 2348–2355. [CrossRef] [PubMed]
9. Olney, S.J.; Griffin, M.P.; Monga, T.N.; McBride, I.D. Work and power in gait of stroke patients. *Arch. Phys. Med. Rehabil.* **1991**, *72*, 309–314. Available online: https://www.archives-pmr.org/article/0003-9993(91)90247-G/fulltext (accessed on 10 June 2022).
10. Parvataneni, K.; Olney, S.J.; Brouwer, B. Changes in muscle group work associated with changes in gait speed of persons with stroke. *Clin. Biomech.* **2007**, *22*, 813–820. [CrossRef]
11. Brincks, J.; Nielsen, J.F. Increased power generation in impaired lower extremities correlated with changes in walking speeds in sub-acute stroke patients. *Clin. Biomech.* **2012**, *27*, 138–144. [CrossRef] [PubMed]
12. Holder, J.; Trinler, U.; Meurer, A.; Stief, F. A Systematic Review of the Associations Between Inverse Dynamics and Musculoskeletal Modeling to Investigate Joint Loading in a Clinical Environment. *Front. Bioeng. Biotechnol.* **2020**, *8*, 603907. [CrossRef] [PubMed]
13. Smith, S.H.L.; Coppack, R.J.; van den Bogert, A.J.; Bennett, A.N.; Bull, A.M.J. Review of musculoskeletal modelling in a clinical setting: Current use in rehabilitation design, surgical decision making and healthcare interventions. *Clin. Biomech.* **2021**, *83*, 105292. [CrossRef] [PubMed]
14. Thelen, D.G.; Anderson, F.C.; Delp, S.L. Generating dynamic simulations of movement using computed muscle control. *J. Biomech.* **2003**, *36*, 321–328. [CrossRef] [PubMed]
15. Bolsterlee, B.; Veeger, D.J.E.; Chadwick, E.K. Clinical applications of musculoskeletal modelling for the shoulder and upper limb. *Med. Biol. Eng. Comput.* **2013**, *51*, 953–963. [CrossRef] [PubMed]
16. Erdemir, A.; McLean, S.; Herzog, W.; van den Bogert, A.J. Model-based estimation of muscle forces exerted during movements. *Clin. Biomech.* **2007**, *22*, 131–154. [CrossRef] [PubMed]
17. Giarmatzis, G.; Jonkers, I.; Wesseling, M.; Van Rossom, S.; Verschueren, S. Loading of Hip Measured by Hip Contact Forces at Different Speeds of Walking and Running. *J. Bone Miner. Res.* **2015**, *30*, 1431–1440. [CrossRef] [PubMed]
18. Smith, C.R.; Won Choi, K.; Negrut, D.; Thelen, D.G. Efficient computation of cartilage contact pressures within dynamic simulations of movement. *Comput. Methods Biomech. Biomed. Eng. Imaging Vis.* **2018**, *6*, 491–498. [CrossRef]
19. Giarmatzis, G.; Fotiadou, S.; Giannakou, E.; Kokkotis, C.; Fanaradelli, T.; Kordosi, S.; Vadikolias, K.; Aggelousis, N. Understanding Post-Stroke Movement by Means of Motion Capture and Musculoskeletal Modeling: A Scoping Review of Methods and Practices. *BioMed* **2022**, *2*, 409–421. [CrossRef]
20. Killen, B.A.; Falisse, A.; De Groote, F.; Jonkers, I. In silico-enhanced treatment and rehabilitation planning for patients with musculoskeletal disorders: Can musculoskeletal modelling and dynamic simulations really impact current clinical practice? *Appl. Sci.* **2020**, *10*, 7255. [CrossRef]
21. Lin, Y.C.; Dorn, T.W.; Schache, A.G.; Pandy, M.G. Comparison of different methods for estimating muscle forces in human movement. *Proc. Inst. Mech. Eng. Part H J. Eng. Med.* **2012**, *226*, 103–112. [CrossRef] [PubMed]
22. Anderson, F.C.; Pandy, M.G. Static and dynamic optimization solutions for gait are practically equivalent. *J. Biomech.* **2001**, *34*, 153–161. [CrossRef] [PubMed]
23. Akbas, T.; Neptune, R.R.; Sulzer, J. Neuromusculoskeletal simulation reveals abnormal rectus femoris-gluteus medius coupling in post-stroke gait. *Front. Neurol.* **2019**, *10*, 301. [CrossRef] [PubMed]
24. Jansen, K.; De Groote, F.; Aerts, W.; De Schutter, J.; Duysens, J.; Jonkers, I. Altering length and velocity feedback during a neuro-musculoskeletal simulation of normal gait contributes to hemiparetic gait characteristics. *J. Neuroeng. Rehabil.* **2014**, *11*, 78. [CrossRef] [PubMed]
25. Roelker, S.A.; Caruthers, E.J.; Hall, R.K.; Pelz, N.C.; Chaudhari, A.M.W.; Siston, R.A. Effects of optimization technique on simulated muscle activations and forces. *J. Appl. Biomech.* **2020**, *36*, 259–278. [CrossRef] [PubMed]
26. Fregly, B.J. A Conceptual Blueprint for Making Neuromusculoskeletal Models Clinically Useful. *Appl. Sci.* **2021**, *11*, 2037. [CrossRef]
27. Balasubramanian, C.K.; Neptune, R.R.; Kautz, S.A. Variability in spatiotemporal step characteristics and its relationship to walking performance post-stroke. *Gait Posture* **2009**, *29*, 408–414. [CrossRef] [PubMed]
28. Kainz, H.; Graham, D.; Edwards, J.; Walsh, H.P.J.; Maine, S.; Boyd, R.N.; Lloyd, D.G.; Modenese, L.; Carty, C.P. Reliability of four models for clinical gait analysis. *Gait Posture* **2017**, *54*, 325–331. [CrossRef] [PubMed]
29. Fotiadou, S.; Aggeloussis, N.; Gourgoulis, V.; Malliou, P.; Papanas, N.; Giannakou, E.; Iliopoulos, I.; Vadikolias, K.; Terzoudi, A.; Piperidou, H. Reproducibility of gait kinematics and kinetics in chronic stroke patients. *NeuroRehabilitation* **2018**, *42*, 53–61. [CrossRef]
30. Seth, A.; Hicks, J.L.; Uchida, T.K.; Habib, A.; Dembia, C.L.; Dunne, J.J.; Ong, C.F.; DeMers, M.S.; Rajagopal, A.; Millard, M.; et al. OpenSim: Simulating musculoskeletal dynamics and neuromuscular control to study human and animal movement. *PLOS Comput. Biol.* **2018**, *14*, e1006223. [CrossRef]

31. Sharifi, M.; Shirazi-Adl, A.; Marouane, H. Sensitivity of the knee joint response, muscle forces and stability to variations in gait kinematics-kinetics. *J. Biomech.* **2020**, *99*, 109472. [CrossRef] [PubMed]
32. Bytyqi, D.; Shabani, B.; Lustig, S.; Cheze, L.; Karahoda Gjurgjeala, N.; Neyret, P. Gait knee kinematic alterations in medial osteoarthritis: Three dimensional assessment. *Int. Orthop.* **2014**, *38*, 1191–1198. [CrossRef] [PubMed]
33. Favre, J.; Clancy, C.; Dowling, A.V.; Andriacchi, T.P. Modification of knee flexion angle has patient-specific effects on anterior cruciate ligament injury risk factors during jump landing. *Am. J. Sports Med.* **2016**, *44*, 1540–1546. [CrossRef] [PubMed]
34. Trinler, U.; Hollands, K.; Jones, R.; Baker, R. A systematic review of approaches to modelling lower limb muscle forces during gait: Applicability to clinical gait analyses. *Gait Posture* **2018**, *61*, 353–361. [CrossRef] [PubMed]
35. Roelker, S.A.; Caruthers, E.J.; Baker, R.K.; Pelz, N.C.; Chaudhari, A.M.W.; Siston, R.A. Interpreting Musculoskeletal Models and Dynamic Simulations: Causes and Effects of Differences between Models. *Ann. Biomed. Eng.* **2017**, *45*, 2635–2647. [CrossRef] [PubMed]
36. Bini, R.; Hume, P. Reproducibility of lower limb motion and forces during stationary submaximal pedalling using wearable motion tracking sensors. *Sport. Biomech.* **2020**, *22*, 1041–1062. [CrossRef] [PubMed]
37. Davis, R.B.; Õunpuu, S.; Tyburski, D.; Gage, J.R. A gait analysis data collection and reduction technique. *Hum. Mov. Sci.* **1991**, *10*, 575–587. [CrossRef]
38. Delp, S.L.; Anderson, F.C.; Arnold, A.S.; Loan, P.; Habib, A.; John, C.T.; Guendelman, E.; Thelen, D.G. OpenSim: Open-source software to create and analyze dynamic simulations of movement. *IEEE Trans. Biomed. Eng.* **2007**, *54*, 1940–1950. [CrossRef]
39. Hamner, S.R.; Seth, A.; Delp, S.L. Muscle contributions to propulsion and support during running. *J. Biomech.* **2010**, *43*, 2709–2716. [CrossRef]
40. Rajagopal, A.; Dembia, C.L.; DeMers, M.S.; Delp, D.D.; Hicks, J.L.; Delp, S.L. Full-Body Musculoskeletal Model for Muscle-Driven Simulation of Human Gait. *IEEE Trans. Biomed. Eng.* **2016**, *63*, 2068–2079. [CrossRef]
41. Delp, S.L.; Loan, J.P.; Hoy, M.G.; Zajac, F.E.; Topp, E.L.; Rosen, J.M. An interactive graphics-based model of the lower extremity to study orthopaedic surgical procedures. *IEEE Trans. Biomed. Eng.* **1990**, *37*, 757–767. [CrossRef]
42. Arnold, E.M.; Delp, S.L. Fibre operating lengths of human lower limb muscles during walking. *Philos. Trans. R. Soc. B Biol. Sci.* **2011**, *366*, 1530–1539. [CrossRef] [PubMed]
43. Thelen, D.G.; Anderson, F.C. Using computed muscle control to generate forward dynamic simulations of human walking from experimental data. *J. Biomech.* **2006**, *39*, 1107–1115. [CrossRef] [PubMed]
44. Virtanen, P.; Gommers, R.; Oliphant, T.E.; Haberland, M.; Reddy, T.; Cournapeau, D.; Burovski, E.; Peterson, P.; Weckesser, W.; Bright, J.; et al. SciPy 1.0: Fundamental algorithms for scientific computing in Python. *Nat. Methods* **2020**, *17*, 261–272. [CrossRef] [PubMed]
45. Growney, E.; Meglan, D.; Johnson, M.; Cahalan, T.; An, K.N. Repeated measures of adult normal walking using a video tracking system. *Gait Posture* **1997**, *6*, 147–162. [CrossRef]
46. Trinler, U.; Schwameder, H.; Baker, R.; Alexander, N. Muscle force estimation in clinical gait analysis using AnyBody and OpenSim. *J. Biomech.* **2019**, *86*, 55–63. [CrossRef] [PubMed]
47. Arnold, E.M.; Hamner, S.R.; Seth, A.; Millard, M.; Delp, S.L. How muscle fiber lengths and velocities affect muscle force generation as humans walk and run at different speeds. *J. Exp. Biol.* **2013**, *216*, 2150–2160. [CrossRef] [PubMed]
48. Lamontagne, A.; Malouin, F.; Richards, C.L.; Dumas, F. Mechanisms of disturbed motor control in ankle weakness during gait after stroke. *Gait Posture* **2002**, *15*, 244–255. [CrossRef] [PubMed]
49. Yavuzer, G.; Öken, Ö.; Elhan, A.; Stam, H.J. Repeatability of lower limb three-dimensional kinematics in patients with stroke. *Gait Posture* **2008**, *27*, 31–35. [CrossRef]
50. Caillet, A.H.; Phillips, A.T.M.; Carty, C.; Farina, D.; Modenese, L. Hill-type computational models of muscle-tendon actuators: A systematic review. *bioRxiv* **2022**. [CrossRef]
51. Borzelli, D.; Pastorelli, S.; Gastaldi, L. Model of the human arm stiffness exerted by two antagoniste muscles. *Adv. Intell. Syst. Comput.* **2017**, *540*, 285–292. [CrossRef]
52. Borzelli, D.; Pastorelli, S.; Gastaldi, L. Determination of the human arm stiffness efficiency with a two antagonist muscles model. *Mech. Mach. Sci.* **2017**, *47*, 71–78. [CrossRef]
53. Sartori, M.; Durandau, G.; Došen, S.; Farina, D. Robust simultaneous myoelectric control of multiple degrees of freedom in wrist-hand prostheses by real-time neuromusculoskeletal modeling. *J. Neural Eng.* **2018**, *15*. [CrossRef] [PubMed]
54. Wang, C.; Jiang, L.; Guo, C.; Huang, Q.; Yang, B.; Liu, H. SEMG-based estimation of human arm force using regression model. In Proceedings of the 2017 IEEE International Conference on Robotics and Biomimetics (ROBIO), Macau, China, 5–8 December 2017; pp. 1–6. [CrossRef]
55. Xiao, F.; Wang, Y.; He, L.; Wang, H.; Li, W.; Liu, Z. Motion Estimation From Surface Electromyogram Using Adaboost Regression and Average Feature Values. *IEEE Access* **2019**, *7*, 13121–13134. [CrossRef]
56. Żuk, M.; Syczewska, M.; Pezowicz, C. Use of the surface electromyography for a quantitative trend validation of estimated muscle forces. *Biocybern. Biomed. Eng.* **2018**, *38*, 243–250. [CrossRef]

57. Karimi, M.T.; Hemmati, F.; Mardani, M.A.; Sharifmoradi, K.; Hosseini, S.I.; Fadayevatan, R.; Esrafilian, A. Determination of the correlation between muscle forces obtained from OpenSim and muscle activities obtained from electromyography in the elderly. *Phys. Eng. Sci. Med.* **2021**, *44*, 243–251. [CrossRef]
58. Giarmatzis, G.; Giannakou, E.; Gkrekidis, A.; Vadikolias, K.; Aggelousis, N. Clinical Validation of Static Optimization during Post Stroke Gait. In Proceedings of the 28th Congress of European Society of Biomechanics, Maastricht, The Netherlands, 9–12 July 2023; Available online: https://esbiomech.org/conference/wp-content/uploads/2023/ESB2023_Book_of_Abstracts.pdf (accessed on 23 January 2024).

Disclaimer/Publisher's Note: The statements, opinions and data contained in all publications are solely those of the individual author(s) and contributor(s) and not of MDPI and/or the editor(s). MDPI and/or the editor(s) disclaim responsibility for any injury to people or property resulting from any ideas, methods, instructions or products referred to in the content.